JOURNAL OF CATALYSIS 8, 14–21 (1967)

Oxidation-Reduction Potentials and Their Relation to the Catalytic Activity of Transition Metal Oxides

K. KLIER

From the Institute of Physical Chemistry, Czechoslovak Academy of Sciences, Prague, Czechoslovakia

Received October 18, 1966, revised January 9, 1967

Calculations of binding energy of oxygen in 3*d* transition metal oxides were carried out on the basis of an ionic model taking into account the crystal field effects. Good agreement was obtained with experimental data concerning variations of binding energy of bulk oxygen in isovalent series. The oxygen binding energy in bulk and on the surface, the free energy of oxidation of lower to higher oxides, and the oxidation-reduction potentials in aqueous media vary with the atomic number of the metal ion according to the same patterns due to the fact that variations of ionization potentials dominate over the variations in crystal field stabilization energy. The extraordinary high oxidation-reduction potential of the Fe^{2+}/Fe^{3+} system explains its relatively low catalytic activity as due to strong oxygen binding. At very low oxidation-reduction potentials (e.g., in Cr^{3+}/Cr^{4+} system) the catalytic activity is also low due to depletion of surface oxygen. Maximum catalytic activity occurs at intermediate (5–20 kcal/mole) oxidation-reduction potentials.

I. Introduction

Oxides of the 3*d* transition elements exhibit characteristic catalytic activity patterns with respect to a number of oxidation-reduction reactions such as oxidation of carbon monoxide (*1–3*), hydrogen (*4*), hydrocarbons (*5*), ammonia (*6*), oxygen exchange reactions (*7*), and nitrous oxide decomposition (*8*). The best catalysts for these reactions are MnO_2, Co_3O_4, CuO, and NiO. The marked feature of the catalytic activity patterns is the rather low activity of iron oxides as compared with oxides of manganese and cobalt (*3*, *9*).

Since a relatively large group of reactions is involved and the results appear to be fairly independent of the method of preparation, we feel justified in attempting a unified interpretation of the regularities described. For this purpose, we shall greatly depend upon the current idea (*9–13*) that the catalytic activity is directly related to the strength of the oxygen bond in the catalyst surface. The first step towards interpretation of catalysis is thus a theoretical treatment of oxygen bond energy.

The present paper deals with the possibilities of calculation of the binding energy of oxygen in bulk and on the surface of oxides. The relation between the bond strength and oxidation-reduction potential of the oxides is determined and the catalytic activity patterns are discussed in terms of these thermochemical quantities.

II. Binding Energy of Oxygen in Ionic Oxides

The binding energy of oxygen is defined here as the standard enthalpy ΔH° of the reaction

$$\frac{1}{n}\,Me_xO_y + \frac{1}{2}\,O_2 \rightarrow \frac{1}{n}\,Me_xO_{y+n} \qquad (1)$$

where the higher oxide represents either bulk or surface compound. Experimental values of ΔH° are tabulated very extensively. However, it is worthwhile to calculate them theoretically in order to find out the reasons

for their variation with atomic number and valency of the metal as well as the structure of the oxides.

The theoretical $\Delta H°$ of reactions (1) can in principle be determined by quantum mechanical calculations of the total energies of Me_xO_y and Me_xO_{y+n}. However, the present state of theory does not allow proceeding much farther than estimation of the overlap integrals between neighboring orbitals (*14*) and some simplified models must be adopted in order to make the theory applicable to experiment. Since it has been recognized that the overlaps in 3*d* metal oxides are small, they can be treated, to a first approximation, as ionic solids (*15*, *16*). We shall use this approximation while taking into account the quantum mechanical effects of inner splitting of 3*d* orbitals in the crystal field of oxygen anions in a way outlined in the work of George and McClure (*17*). In a parallel work (*18*) we have shown that the lattice energies of 3*d* metal oxides are very well accounted for by the above model so that the idealization of ionic binding is sufficiently realistic within the group of compounds studied.

Similarly as in ref. (*18*) the enthalpy of reaction (1) can be calculated from the Born-Haber cycle as follows:

$$\Delta H° = -\frac{1}{n} U_t(Me_xO_y) + \frac{1}{n} U_t(Me_xO_{y+n}) + \frac{1}{2} D_{O_2} - E_{O^{2-}} + E_I \quad (2)$$

where U_t are the respective theoretical lattice energies, D_{O_2}, the dissociation energy of the oxygen molecule, $E_{O^{2-}}$, the electron affinity of an oxygen atom towards two electrons, and E_I, the energy of formation of a cation of higher valency from one of lower valency. In most cases valency changes by unity and

$$E_I = 2I^*_{1+2y/x,\ 298}$$

$I^*_{k,298}$ is the kth ionization potential corrected for 298°K and the valence state preparation energy (*17*).

The calculations were made for the reaction

$$3FeO + \tfrac{1}{2}O_2 \rightarrow Fe_3O_4$$

with the results $\Delta H° = -104$ kcal/mole for $U_t(FeO) = -955.5$ kcal/mole and $\Delta H° = -157$ kcal/mole for $U_t(FeO) = -938$ kcal/mole, the $U_t(Fe_3O_4)$ being equal to 4611 kcal/mole [all these data from ref. (*18*)]. When these values are compared with the experimental value $\Delta H° = -76$ kcal/mole, it is seen that although lattice energies can be calculated with 1% accuracy (*18*), this is not enough for sufficiently accurate calculations of $\Delta H°$.

However, if only variations of $\Delta H°$ in series of isovalent and isostructural oxides are to be determined, the calculation of the total lattice energy can be circumvented as follows.

The difference of lattice energies

$$\Delta U = -U_t(Me_xO_y) + U_t(Me_xO_{y+n})$$

would be a monotonous function of atomic number of cation in an isovalent and isostructural series, were the crystal field effects absent (*24*). ΔU can thus be divided into a monotonous part ΔU_0 and a part involving the crystal field effects, $\Delta E_c{}^t$

$$\Delta U = \Delta U_0 + \Delta E_c{}^t$$

where $\Delta E_c{}^t$ is the so-called thermodynamic stabilization energy (*18*). It is usually slightly higher (*17*) than its optical counterpart ΔE_c, which is probably due to the lower repulsion potential of nonspherically symmetrical *d*-electron configurations (*18*). For practical calculation no difference will be made between these two quantities.

Equation (2) can thus be rewritten

$$\Delta H° = \frac{1}{n}\Delta U_0 + \frac{1}{n}\Delta E_c + \frac{1}{2} D_{O_2} - E_{O^{2-}} + E_I \quad (3)$$

where only ΔE_c and E_I exhibit periodic variations with cation atomic number. We shall illustrate these variations on systems where divalent ion becomes oxidized to trivalent. The values of E_I are determined by the third ionization potentials which are graphically represented by a dashed curve in Fig. 1. The relative stability with respect to ionization of d^5 and d^{10} systems is due to maximum multiplicity stabilization (Hund's rule) for five unpaired electrons and the

closed-shell stabilization, respectively. These rules also hold for other ionization potentials (see, e.g., Fig. 2) and in other transition series.

Before proceeding to quantitative estimates of ΔE_c, we shall show that stabilization by crystal field opposes that by maximum multiplicity. Consider oxidation of Mn^{2+} (d^5, $E_c = 0$) to Mn^{3+} (d^4, $E_c < 0$) as compared with oxidation of Fe^{2+} (d^6, $E_c < 0$) to Fe^{3+} (d^5, $E_c = 0$) in any symmetry of

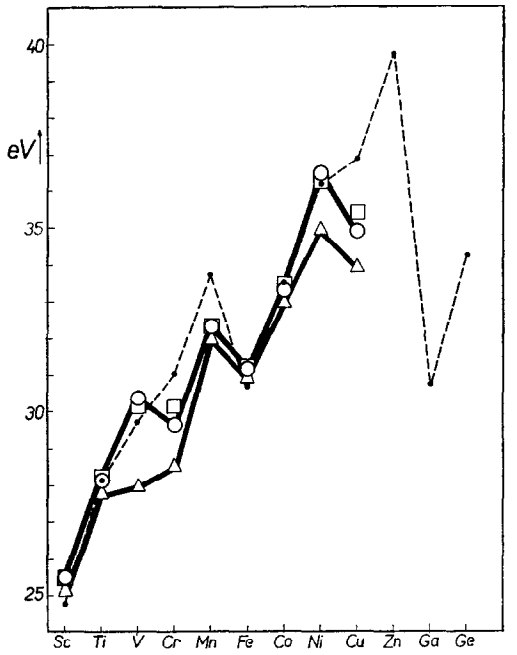

FIG. 1. Variations of the third ionization potentials (*20*) corrected for crystal field effects. Dashed curve, $I^*_{3,298}$; $I^*_{3,298} + \Delta E_c$: O, bulk reactions (4) and (5), □, oxygen chemisorption on (100) plane of B1 MeO oxides, △, oxygen chemisorption on (110) plane of B1 MeO oxides.

weak crystal fields. The oxidation of Mn^{2+} to Mn^{3+} is made easier by the crystal field stabilization of Mn^{3+} but thwarted by maximum multiplicity stabilization of Mn^{2+} while the opposite holds for iron. The difference of the third ionization potentials of Mn and Fe is about 90 kcal/mole whereas the difference in crystal field stabilization energies amounts to some 30–50 kcal/mole, according to structure. This is an example of a quite general rule that in weak fields the enthalpy of these red-ox reactions follows the domi-

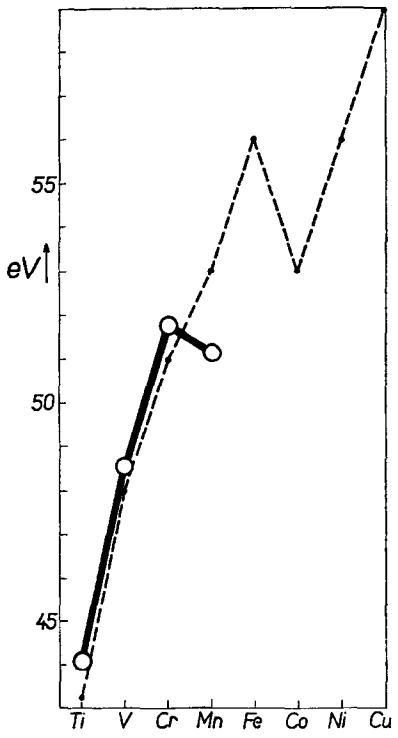

FIG. 2. Variations of the fourth ionization potentials (*20*) corrected for crystal field effects. Dashed curve, $I^*_{4,298}$, O, $I^*_{4,298} + \Delta E_c$ for bulk reactions (6).

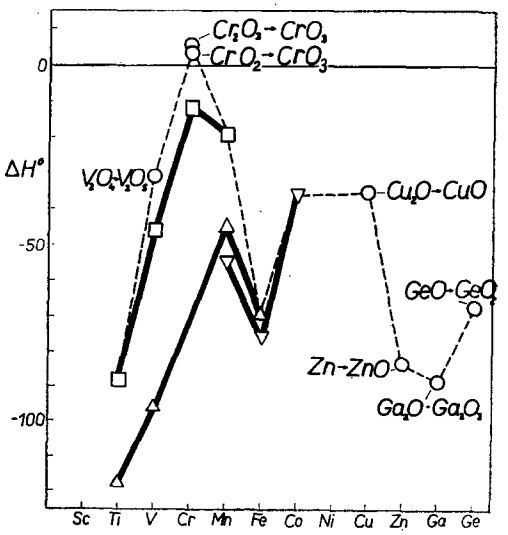

FIG. 3. Standard enthalpy changes $\Delta H°$ of oxidation of lower to higher oxides: O, most stable systems, ▽, reaction (4), △, reaction (5), □, reaction (6).

TABLE 1
HEATS OF REACTION, STANDARD FREE ENERGY AND ENTROPY CHANGES IN OXIDATIONS OF LOWER TO HIGHER OXIDES[a]

No	Reaction	$-\Delta F°_{300}$	$-\Delta S°_{300}$	$-\Delta F°_{600}$	$-\Delta S°_{600}$	$-\Delta H°_{300}$[b]	$-\Delta H°_{300}$[c]
1	$2TiO \rightarrow Ti_2O_3$	108 607	21.65	102 120	19.49	115 102	119 176
2	$Ti_2O_3 \rightarrow 2TiO_2$	82 095	20.07	76 310	21.01	88 116	69 000
3	$2VO \rightarrow V_2O_3$	90 082	19.69	84 251	19.23	95 989	90 000
4	$V_2O_3 \rightarrow V_2O_4$	38 964	23.44	33 505	17.01	45 996	54 000
5	$V_2O_4 \rightarrow V_2O_5$	25 636	17.94	18 917	23.17	31 018	29 000
6	$Cr_2O_3 \rightarrow 2CrO_2$	6 810	18.77	690	21.35	12 441	15 300
7	$CrO_2 \rightarrow CrO_3$	−9 239	21.76	−13 828	7.32	−2 711	—
8	$\frac{1}{2}(Cr_2O_3 \rightarrow 2CrO_3)$	−11 668	20.76	−26 966	12.13	−5 440	3 293
9	$3MnO \rightarrow Mn_3O_4$	45 752	31.83	36 173	31.80	55 301	55 400
10	$2MnO \rightarrow Mn_2O_3$	37 141	26.66	29 069	26.75	45 129	48 000
11	$Mn_2O_3 \rightarrow 2MnO_2$	11 769	25.62	4 167	25.11	19 455	16 900
12	$3FeO \rightarrow F e_3O_4$	66 959	31.48	57 307	30.71	76 403	75 900
13	$2FeO \rightarrow Fe_2O_3$	59 869	31.13	50 475	30.66	69 208	69 100
14	$3CoO \rightarrow Co_3O_4$	27 066	29.79	18 377	26.14	36 003	38 400
15	$Cu_2O \rightarrow 2CuO$	26 868	26.53	19 083	25.39	34 827	34 360
16	$\frac{1}{2}(Ga_2O \rightarrow Ga_2O_3)$	80 524	24.93	72 850	26.12	88 003	88 000
17	$GeO \rightarrow GeO_2$	60 821	21.58	54 287	21.81	67 295	—
18	$Zn \rightarrow ZnO$	76 032	24.04	68 927	23.41	83 244	83 170

[a] All values of $\Delta F°$ and $\Delta H°$ are in cal/g atom of oxygen, values of $\Delta S°$ in entropy units.
[b] Calculated from $\Delta F°_{300}$ and $\Delta S°_{300}$.
[c] Calculated from data in ref. (*19*).

nant variations of ionization potentials corrected by smaller but not negligible ΔE_c values.

The above considerations are confirmed by experimental enthalpy changes corresponding to reaction (1) as demonstrated in Fig. 3 and Table 1. This figure comprises three series of reactions, viz.,

$$3MeO + \tfrac{1}{2}O_2 \rightarrow Me_3O_4 \quad (Me = Mn, Fe, Co) \qquad (4)$$

$$2MeO + \tfrac{1}{2}O_2 \rightarrow Me_2O_3 \quad (Me = Ti, V, Mn, Fe) \qquad (5)$$

$$Me_2O_3 + \tfrac{1}{2}O_2 \rightarrow 2MeO_2 \quad (Me = Ti, V, Cr, Mn) \qquad (6)$$

The reactions of other stable oxides are also given. As expected, heats of reactions (4) and (5) follow the variations of third ionization potentials modified by crystal field stabilization energy changes, as demonstrated by the course of $I^*_{3,298} + \Delta E_c$ in Fig. 1,* with a local minimum at Fe^{2+}/Fe^{3+} system. Enthalpies of reactions (6) follow the course of the fourth ionization potentials modified by the corresponding crystal field stabilization energy changes. The extraordinary high crystal field stabilizations of d^3 systems (Cr^{3+} and Mn^{4+}) project themselves in the local maximum at Cr^{3+}/Cr^{4+} system (see also the course of $I^*_{1,298} + \Delta E_c$ in Fig. 2*).

In these considerations the differences in lattice energies due to the various structural deformations were not taken into account.

* ΔE_c values were calculated assuming that crystal fields are in all oxides weak and strictly octahedral, taking Dq as in ref. (*18*). This is a rough approximation since octahedral symmetry is distorted especially in sesquioxides and dioxides, but only a small error is introduced in ground state energies. For spinels Me_3O_4 cation distribution among tetrahedral and octahedral sites was respected, namely $Me_{tet}^{2+}(Me^{3+})_{2,oct}$ in the normal spinels Mn_3O_4 and Co_3O_4, and Me_{tet}^{3+} Me_{oct}^{2+} Me_{oct}^{3+} in the inversion spinel Fe_3O_4. ΔE_c is related always to one Me^{3+}. For Co^{3+} in Co_3O_4 and V^{3+} in V_2O_3 the strong field approximation is a better physically justified one because Co_3O_4 is diamagnetic and $V(H_2O)_6^{3+}$ has a spectrum which corresponds to the strong field case (*21*). However, when pairing energy is taken into account, the stabilization is only by about 0.1 eV stronger than in the weak field limit.

These effects are such as to minimize the crystal energy; they are therefore responsible for the fact that variations in ΔH° observed are smaller than those of $I^*_{3,298} + \Delta E_c$.

Surface reactions can be treated similarly. For example, oxygen chemisorption according to

$$Me^{2+} + \tfrac{1}{2}O_2 \rightarrow Me^{3+} + O^-_{ads} \qquad (7)$$

has the enthalpy

$$\Delta H^\circ_s = I^*_{3,298} + \Delta E_c + \Delta U_{0,s} + \tfrac{1}{2}D_{O2} - E_O \qquad (8)$$

Periodic variations of this quantity are again given by variations of $I^*_{3,298} + \Delta E_c$. We shall consider oxygen chemisorption* on the (100) and (110) planes of B1 oxides, according to Haber and Stone (*22*). The (111) plane is not taken into account because it does not appear as a cleavage plane in the surface of ionic crystals (*23*). The values of $I^*_{3,298} + \Delta E_c$ for (100) plane† are almost the same as those for bulk oxidations and those for the (110) plane‡ follow a more or less parallel course (Fig. 1).

There emerges the important result that the oxygen bond strength patterns are similar for various geometrical models and even for surface and bulk oxygen. A characteristic feature is a local minimum at the Fe^{2+}/Fe^{3+} system showing the increased stability of the oxidized state owing to relatively easy ionization of the d^6 system. It should be noted that the above results apply only for the 3*d* oxides while the model fails for 4*d* oxides and 3*d* sulfides owing to the large proportion of "covalent" bonding.

III. Oxidation-Reduction Potentials

The quantity $I^*_{3,298} + \Delta E_c$ from Fig. 1 as well as ΔH° of reactions (4) and (5) exhibit patterns similar to that of the standard free energy change of the reaction (*17*)

$$Me_{aq}^{2+} + H^+ \rightarrow Me_{aq}^{3+} + \tfrac{1}{2}H_2$$

The negative value of this quantity is the oxidation-reduction potential of the Me^{2+}/Me^{3+} system related to the hydrogen electrode.

For solid oxides the oxidation-reduction potential may be defined in an analogous way as the standard free energy change, $-\Delta F^\circ_T$, of reaction (1). This quantity was calculated from data in tables of ref. (*25*) and its values are presented together with the corresponding enthalpy and entropy changes in Table 1. The dependence of ΔF°_{300} on ΔH° is shown in Fig. 4. As earlier pointed out by Tanaka and Tamaru (*26*), this dependence is fairly linear. The same shows the ΔF°_{600} vs. ΔH° graph but for an additional constant. The small variations of entropy changes, which are responsible for these linear relationships, indicate similarity of the character of the oxygen bond in various oxides (*27*). The oxidation-reduction potentials of oxides are thus determined, but for a constant (about 7 kcal/mole at 300°K and 14 kcal/mole at 600°K), by the binding energy of oxygen and therefore can in principle be calculated from Madelung energies, ionization potentials, and crystal field stabilization energies.

IV. The Relation between Catalytic Activity and Oxidation-Reduction Potentials

The oxidation-reduction reactions (e.g., those listed in Section I) are generally assumed to proceed by a stepwise mechanism

(a) $A + K\text{-ox} \rightarrow AO_{ads} + K\text{-red}$

(b) $AO_{ads} \rightarrow AO_g$

(c) $K\text{-red} + \tfrac{1}{2}O_2 \rightarrow K\text{-ox}$

where K-ox and K-red are the oxidized and reduced states of the catalyst, A the substrate, and AO the product of oxidation. Process (a) is in our case reaction of substrate with chemisorbed or lattice oxygen; (b) is desorption of product from the catalyst surface; and (c) is reoxidation of the catalyst by gaseous oxygen. In the reaction phases

* Chemisorbed oxygen is considered equivalent to bulk oxygens and therefore probably the highest ΔE_c estimates are made.

† ΔE_c for the (100) plane was calculated for the transition Me^{2+} (square pyramid) $\rightarrow Me^{3+}$ (octahedron) in a way similar to that of Dowden and Wells (*24*). However, a weak field approximation was used without exception for d^2 and d^7 in ref. (*24*).

‡ ΔE_c for (110) calculated for the transition $\frac{1}{2}$[3Me^{2+} (tetrahedron) $\rightarrow Me^{2+}$ (square pyramid) + Me^{3+} (octahedron) + Me^{3+} (square pyramid)]. All weak fields.

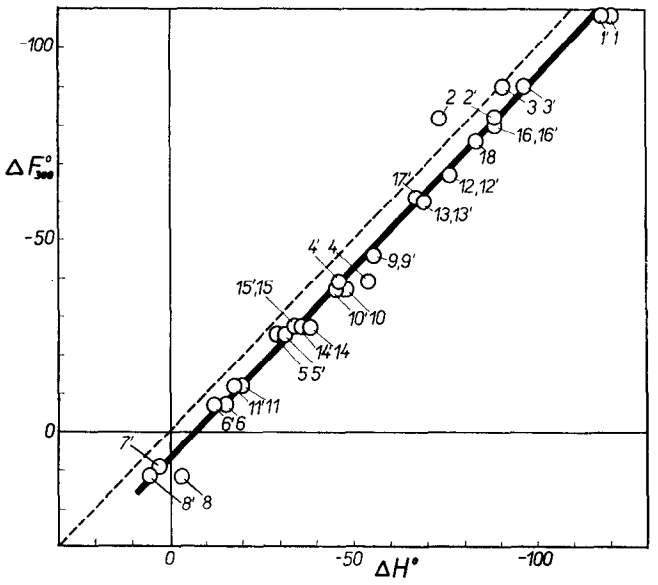

FIG. 4. Standard free energy ΔF°_{300} vs. standard enthalpy ΔH° plot for oxidation of lower to higher oxides. Numbers correspond to reactions in Table 1. Primes denote enthalpies ΔH°_{300},[b] numbers without primes denote enthalphies ΔH°_{300}[c] from Table 1.

(a) and (c) may be involved a number of further intermediate steps such as adsorption of reactants, etc.

For discussion of catalytic activity it is useful to distinguish between two temperature regions: (1) the low-temperature one (for oxides $-80°$ to $+100°$C) in which the slow desorption of reaction products or adsorption of reactants may considerably influence the overall reaction rate; (2) the high-temperature region (for oxides above 150–200°C) in which adsorption–desorption processes are substantially faster and the overall rate is determined by the rate of steps (a) and/or (c).

Carbon monoxide oxidation may serve as an example of the complexity of the reaction mechanism in Region (1). On basic oxides such as MnO, CoO, and NiO the most difficult step at 20°C is CO_2 desorption, while on "neutral" MnO_2 it is the chemisorption of oxygen on a reduced surface (*28*, *29*). Under these conditions it is difficult to correlate the total activity of different catalysts with a single energy parameter. On the other hand, in Region (2) it is quite likely that the oxidation-reduction reactions (a) and (c) are rate-determining. For this case it appears feasible to correlate the catalytic activity with the oxidation-reduction potential of the oxides $-\Delta F^\circ_T$ which is, as already mentioned, well approximated by the enthalpy of oxidation ΔH°. The correlations between the logarithm of the rate of oxidation-reduction reactions, log W, and ΔH were constructed in the very thorough review of Golodets and Roiter (*13*). They exhibit a maximum of rate for the catalytic systems Co_3O_4/CoO, Cu_2O/CuO, and MnO_2/Mn_2O_3 at ΔH° about -20 kcal/mole for oxidation of hydrogen and about -35 kcal/mole for oxidation of carbon monoxide. When using ΔF°_{600} the maximum is only a little above the zero oxidation-reduction potential (Fig. 5). Similarly as in Golodets and Roiter's work, the covalent V_2O_5 with several kinds of V–O bonds (*30*) falls out of the correlation.

The maximum on the log W vs. ΔH° curve was discussed by a number of authors. We shall, therefore, restrict ourselves to its qualitative interpretation in terms of oxidation-reduction potentials of the oxides. In the region to the left of the maximum on Fig. 5 the energy effects dominate: the more negative is ΔF, the stronger is oxygen binding and the slower becomes reaction (a). [It is assumed with Boreskov (*9*) that activation

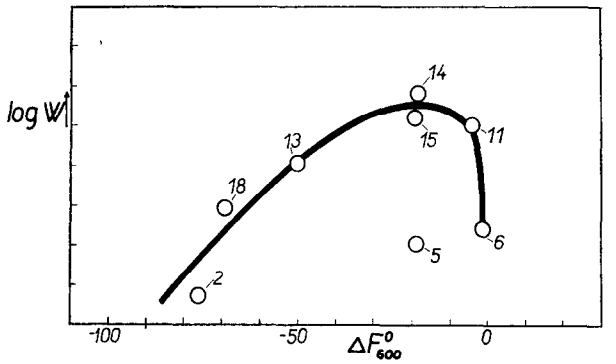

FIG. 5. Relation between catalytic activity, log W, for oxidation of hydrogen (*4*, *13*) and the oxidation-reduction potential of oxides at 600°K, $-\Delta F^\circ_{600}$. The numbering of catalytic systems is the same as in Table 1.

energy of this reaction is proportional to the strength of the oxygen bond.] To the right of the maximum concentration effects prevail: the oxygen is weakly bonded and therefore highly reactive as in CrO_2 and CrO_3, but around and beyond $\Delta F^\circ_T = 0$ its equilibrium concentration strongly decreases. In the stationary state its concentration will be yet smaller than the equilibrium one and reaction (a) again becomes slow, in this case due to exhaustion of K-ox. Hence the low activity of Cr_2O_3 in which the surface oxygen is practically stripped off the surface.

It is shown above that the values of ΔF°_T are parallel to those of ΔH° and that the patterns for surface reactions are qualitatively the same as those for bulk reactions. This gives a reasonable background for the existing correlation between bulk oxidation-reduction potentials and the rate of surface catalytic reaction. The patterns in isovalent series are thus explained essentially by an ionic model taking into account the crystal field effects. For example, the relatively low activity of the Fe^{2+}/Fe^{3+} system stems from the relative stability of the oxidized state due to the low third ionization potential of iron. However, the absolute values of oxidation-reduction potentials cannot be determined at present because of lack of structural data and insufficient accuracy of the determination of lattice energy.

The ionic character of bonding is probably also responsible for the small selectivity of the oxides towards deep oxidation of various substrates. Process (a) can be schematically written for the various reactions as follows:

$$H_2 + O^{\delta-} \rightarrow H_2O + \delta\ominus$$
$$CO + O^{\delta-} \rightarrow CO_2 + \delta\ominus$$
$$CH_4 + 4O^{\delta-} \rightarrow CO_2 + 2H_2O + 4\delta\ominus$$
$$N_2O \rightarrow N_2 + O^{\delta-} \rightarrow N_2 + \tfrac{1}{2}O_2 + \delta\ominus$$
$$O^{\delta-} \rightarrow \tfrac{1}{2}O_2 + \delta\ominus \text{ desorption of oxygen, reaction step in oxygen exchange}$$
$$2NH_3 + 5O^{\delta-} \rightarrow 2NO + 3H_2O + 5\delta\ominus$$

$O\delta^-$ is a symbol for surface lattice or chemisorbed oxygen anions and $\ominus$, for electrons which may undergo subsequent reactions such as reduction of cations, neutralization of excess positive charges (holes) in the oxide, localization at defects, etc. The first step is, however, always of the same type. The substrates always react with the same oxygen anions whose bond energy and concentration exhibit similar patterns in the series of the oxides under consideration. The differences in reaction rates of various substrates with oxygen anions then cause only a constant shift of the activity patterns. The above considerations do not hold for strongly covalent oxides such as V_2O_5, which in fact exhibits an exceptional behavior.

REFERENCES

1. NEUMANN, B., KRÖGER, C., AND IWANOWSKI, R., *Z. Elektrochem.* **37**, 121 (1931).
2. STONE, F. S., *Advan. Catalysis* **13**, 1 (1962).
3. KRYLOV, O. V., *Kinetika i Kataliz* **3**, 502 (1962).
4. POPOVSKII, V. V., AND BORESKOV, G. K., *Probl. Kinetiki i Kataliza, Akad. Nauk USSR* **10**, 67 (1960).

5. GERALD, N. G., AND HORWATITSCH, H., *Mikrochim. Acta* (No. 1-2) 7 (1962); KAINZ, G., AND HORWATITSCH, H., *ibid.*, p. 16.
6. KLISSOURSKI, D. G., KYNEV, S., AND VATEVA, E., *Commun. Phys. Inst. Bulgarian Acad. Sci.* **9**, 57 (1962).
7. DZISYAK, A. P., BORESKOV, G. K., AND KASATKINA, L. A., *Kinetika i Kataliz* **3**, 81 (1962).
8. SAITO, Y., YONEDA, Y., AND MAKISHIMA, S., *Actes Congr. Intern. Catalyse, 2e, Paris, 1961*, p. 1937 (1962).
9. BORESKOV, G. K., *Advan. Catalysis* **15**, 285 (1964).
10. RIENÄCKER, G., *Z. Chem.* **3**, 121 (1963).
11. SACHTLER, W. M. H., AND DE BOER, N. H., *Proc. Intern. Congr. Catalysis, 3rd, Amsterdam, 1965*, p. 252 (1966).
12. MAKISHIMA, S., YONEDA, Y., AND SAITO, Y., *Actes Congr. Intern. Catalyse, 2e, Paris, 1961*, p. 617 (1962).
13. GOLODETZ, G. I., AND ROITER, V. A., *Ukr. Khim. Zh.* **29**, 667 (1963).
14. MORIN, F. J., *J. Appl. Phys. Suppl.* **32**, 2195 (1961).
15. MORIN, F. J., *Bell System Tech. J.* **37**, 1047 (1958).
16. KLIER, K., *Chem. Listy* **58**, 621 (1964).
17. GEORGE, P., AND MCCLURE, D. S., *Progr. Inorganic Chem.* **1**, 381 (1959).
18. KLIER, K., Lattice energies of transition metal oxides, *Coll. Czech. Chem. Commun.*, in press.
19. "Selected Values of Chemical Thermodynamic Properties." *Natl. Bur. Std. U. S. Circ.* **500** (1952).
20. VON ARDENNE, M., "Tabellen der Elektronenphysik, Ionenphysik und Utebermikroskopie." I Band, p. 479, Deutscher Verlag der Wissenschaften, Berlin, 1956.
21. BALLHAUSEN, C. J., "Ligand Field Theory." McGraw-Hill, New York, 1962.
22. HABER, J., AND STONE, F. S., *Trans. Faraday Soc.* **59**, 192 (1963).
23. WOLFF, G. A., *Proc. Intern. Symp. on Reactivity of Solids, Gothenburg, 1952*, p. 253.
24. DOWDEN, D. A., AND WELLS, D., *Actes Congr. Intern. Catalyse, 2e, Paris, 1961*, p. 1499 (1962).
25. *U. S. Bureau of Mines, Bull.* **542** (1954).
26. TANAKA, K. I., AND TAMARU, K., *J. Catalysis* **2**, 366 (1963).
27. KUBASCHEWSKI, O., AND EVANS, E., "Metallurgical Thermochemistry," 2nd ed., p. 193. Pergamon Press, London, 1955.
28. NAJBAR, M., KUCHYNKA, K., AND KLIER, K., *Coll. Czech. Chem. Commun.* **31**, 959 (1966).
29. KLIER, K., AND KUCHYNKA, K., *J. Catalysis* **6**, 62 (1966).
30. TARAMA, K., TERANISHI, S., YOSHIDA, S., AND TAMURA, N., *Proc. Intern. Congr. Catalysis, 3rd, Amsterdam, 1964*, p. 282 (1965).